Effects of Macromolecular Crowding on the Conformational Ensembles of Disordered Proteins

*Sanbo Qin and Huan-Xiang Zhou**

Department of Physics and Institute of Molecular Biophysics, Florida State University, Tallahassee, FL 32306, USA

Supporting Information

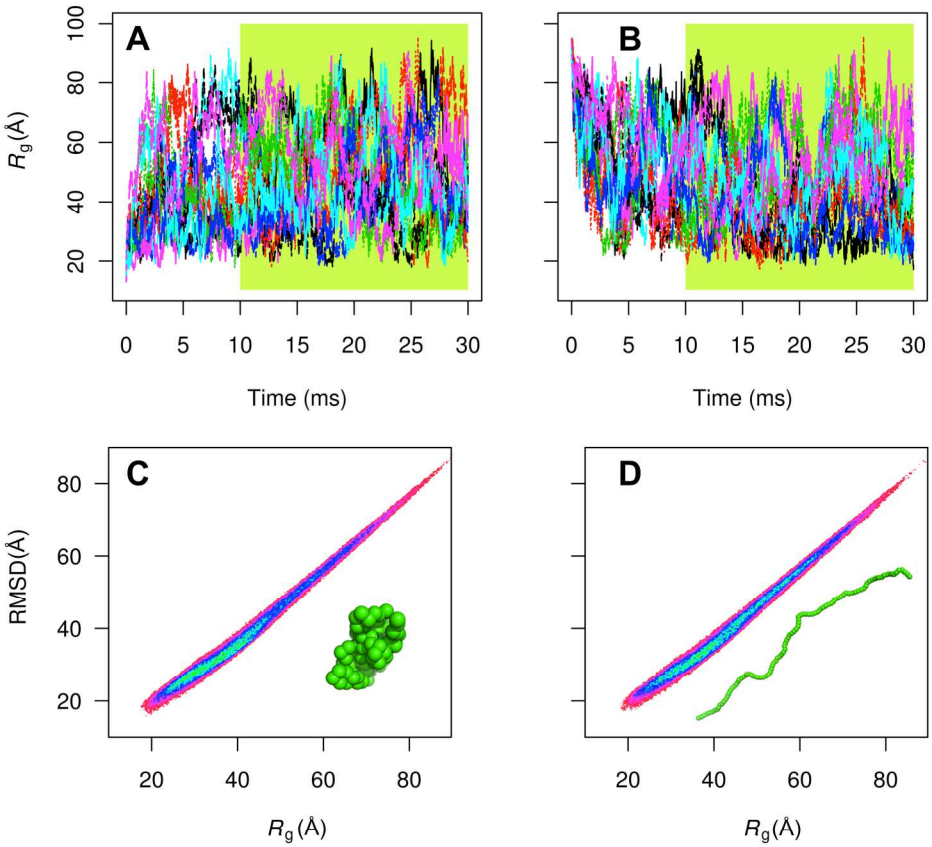

Figure S1. Comparison of conformational sampling in two sets of trajectories (ξ = 0.7). Each set consists of 36 repeat trajectories that were started either from a compact (panels **A** and **C**) or an extended (panels **B** and **D**) conformation for the IDP. (**A**) and (**B**) Instantaneous R_g values along the 36 trajectories. Shaded regions are used for calculating averages. (**C**) and (**D**) 2-d histograms in R_g and RMSD; the latter refers to root-mean-square-deviation from the compact initial conformation.

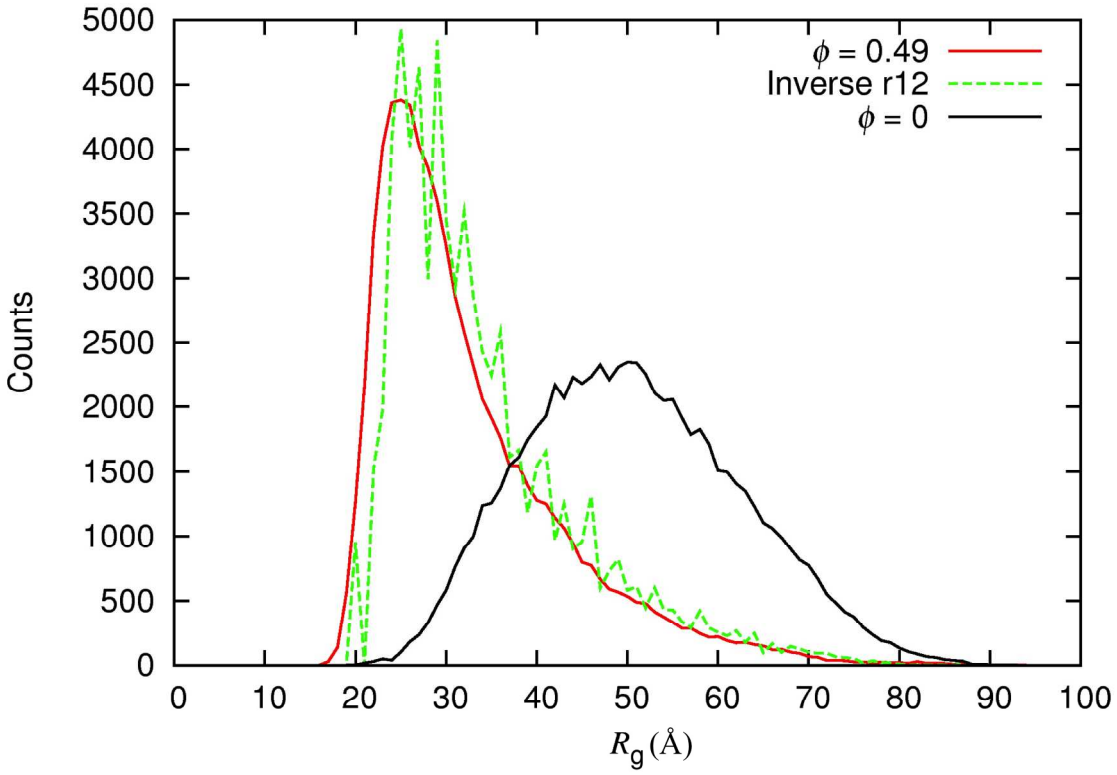

Figure S2. Histograms of R_g from direct simulations at $\phi = 0.49$ and predicted by postprocessing the crowder-free simulations (with $\phi = 0$), with $\Delta\mu$ calculated by exact treatment of the inverse r^{12} form of protein-crowder interactions. Under-sampling of conformations with R_g around 20 Å by the crowder-free simulations leads a slight overestimate of $R_{g;rms}$.

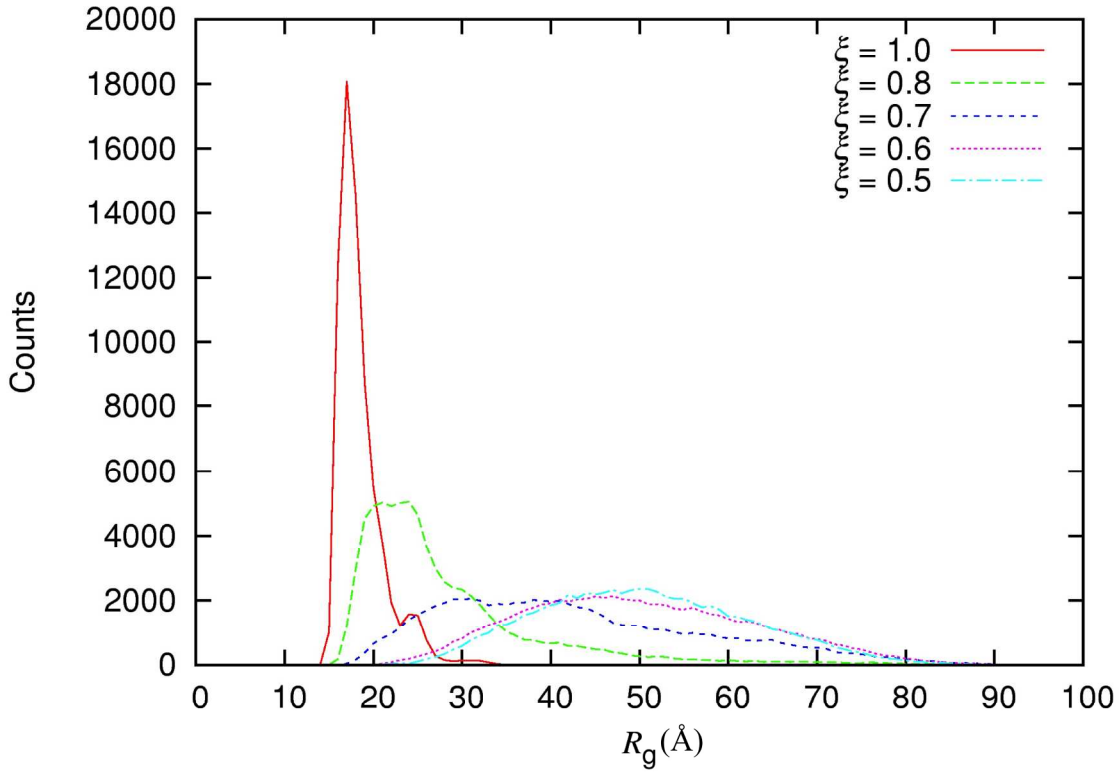

Figure S3. Histograms of R_g for the IDP with different ξ at $\phi = 0$.

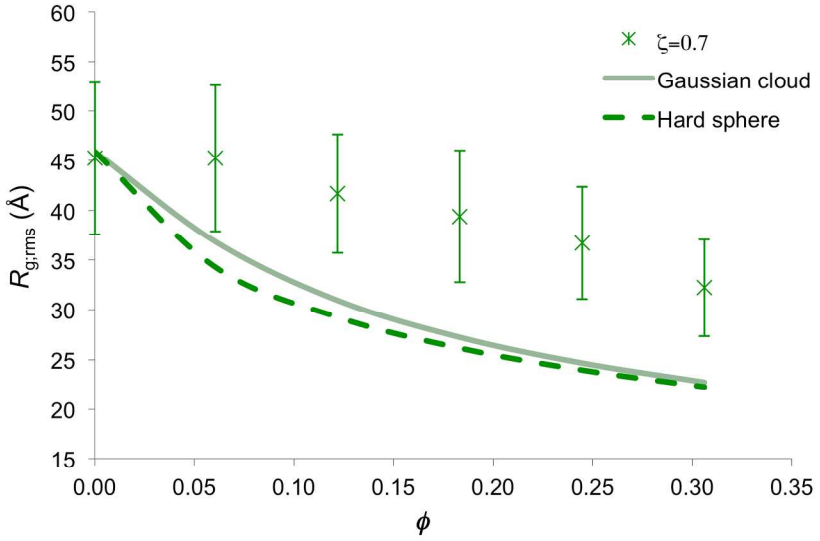

Figure S4. Comparison of $R_{g;rms}$ obtained from the direct simulations at $\xi = 0.7$ and predicted by the Gaussian cloud and equivalent hard sphere models of Minton.

TABLE S1: Standard Deviations of R_g (in Å) After Combining 36 Direct-Simulation Trajectories

ξ \ ϕ	0.00	0.06	0.12	0.18	0.24	0.31	0.37	0.43	0.49
1.0	2.6	2.4	2.4	2.3	2.1	2.2	2.4	1.8	1.5
0.8	10.6	8.2	8.0	7.8	6.7	4.3	4.3	3.4	2.8
0.7	14.8	15.3	13.5	13.2	12.6	10.6	8.8	5.7	4.3
0.6	12.9	12.8	13.5	13.7	13.7	12.9	11.6	9.3	7.1
0.5	11.8	11.8	11.9	12.1	12.6	11.9	12.0	10.3	10.4